RSC Advances

Temperature sensitive optical properties of exciton and room-temperature visible light emission from disordered Cu2O Nanowires

Journal:	*RSC Advances*
Manuscript ID:	RA-COM-06-2014-005595.R1
Article Type:	Communication
Date Submitted by the Author:	03-Aug-2014

Complete List of Authors:	Wang, Peng; Institute of Microelectronics, School of Physical Science and Technology, Lanzhou University Zhao, Xinhong; Department of Optical Information Science and Technology, School of Mechanical Engineering,Jiangsu University Li, Hairong; Institute of Microelectronics, School of Physical Science and Technology, Lanzhou University Li, Lingshan; OriginLab (Guangzhou) Ltd., Li, Jing; Maternity & Child-care Hospital of Gansu province, Ma, Guofu; Institute of Microelectronics, School of Physical Science and Technology, Lanzhou University Chang, Jingxian; Institute of Microelectronics, School of Physical Science and Technology, Lanzhou University

RSC Advances

RSCPublishing

COMMUNICATION

Temperature sensitive optical properties of exciton and room-temperature visible light emission from disordered Cu_2O Nanowires

Cite this: DOI: 10.1039/x0xx00000x

Received 00th January 2012,
Accepted 00th January 2012

DOI: 10.1039/x0xx00000x

www.rsc.org/

Peng Wang,[a*] Xinhong Zhao,[b] Hairong Li,[a] Lingshan Li,[c] Jing Li,[d] Guofu Ma,[a] and Jingxian Chang[a]

Disordered Cu_2O nanowires (NWs) were prepared by a two-step growth method. Photoluminescence properties of Cu_2O NWs have been investigated in detail. The excitonic optical properties from the Cu_2O NWs are temperature sensitive. At room temperature, a longitudinal optical (LO) phonon replica and visible light emission from exciton recombination were observed for the first time.

Introduction

In recent years, semiconductor nanostructures have attracted more and more research interests. As a typical p-type direct band gap semiconductor within 2.0-2.2 eV [1-3], cuprous oxide (Cu_2O) nanostructures have been regarded as ideal candidates in solar energy conversion [4,5]. Furthermore, due to its large exciton binding energy with 150 meV [6] and long-lived exciton lifetime of ~10 microseconds [3], it is also an excellent candidate to realize excitonic devices [7]. A series of methods of the Cu_2O nanostructures fabrication with well morphologies, such as cages, cubes, wires and yolk-shell structures, have been presented [8-11]. Among these nanostructures, Cu_2O nanowires(NWs) extraordinarily appeals to researchers due to their one dimensional architecture for promising applications as photocatalysis, optoelectronics, and power strorage [10,12,13]. However, to the best of our knowledge, few studies about the optical properties of band edge exciton in Cu_2O NWs have been reported. Furthermore, the emission from the lowest direct bandgap exciton in Cu_2O thin films is hardly observed due to its dipole-forbidden, and the signal from the dipole-allowed exciton is too weak to be measured [14]. Therefore, the studies of the exciton emission with dipole-allowed or dipole-forbidden in Cu_2O NWs are seldom reported. Thus the advance in nanowire-based cuprous oxides has attracted much interest in exploiting their direct recombination from near band edge exciton or exciton emission with phonon-assisted. In this work, a two-step growth method for synthesizing pod-like Cu_2O NWs is presented. And the excitonic optical properties near band edge of Cu_2O NWs sample are investigated systematically. Weak exciton emission lines are observed in low temperature photoluminescence (PL) spectra, and the first-order longitudinal optical (LO) phonon replica appears on room temperature PL spectra. More importantly, an obvious visible light emission is observed in this work. Our study would advance the understanding of exciton-related emission in Cu_2O NWs. Since phonon anticipated exciton emission can be used to tailor the exciton−phonon coupling strength of nanoscale excitons, it would large extent optimize the optical properties of exciton related devices (such as charge carrier mobility, exciton relaxation and lifetimes). Therefore, the structure of Cu_2O NWs should have great potential applications in the development of NW-based optoelectronic devices.

Results and discussion

The synthesis of Cu_2O NWs includes two steps. The first step involves the fabrication process of $Cu(OH)_2$ NWs: First, 25 ml 0.125 M ammonium persulfate ($(NH_4)_2S_2O_8$) and 25 ml 2.5 M sodium hydroxide (NaOH) was mixed and stirred at room temperature. A copper foil was cleaned followed by the method of our previous work [15]. Then the cleaned copper foil substrate was placed into the mixture with NaOH and$(NH_4)_2S_2O_8$. After 30 minutes, $Cu(OH)_2$ NW arrays were obtained on the surface of the copper substrate. In the second step, $Cu(OH)_2$ NW arrays were annealed using muffle furnace in two different temperatures. After 1 hour, Cu_2O NWs were obtained from the prepared $Cu(OH)_2$ NWs. The detailed fabricated process of Cu_2O NWs is reported in our recent work [16].

In a typical experiment, Cu_2O NWs are obtained using the method mentioned above. Top view scanning electron microscopy (SEM) images of typical Cu_2O NWs are shown in Figure 1a and b. In Figure 1a, the diameter of NWs is in the range of 95−190 nm, the length of them range from 10 to 25 μm. It is noted that the NWs show slight curved and the bulges appear on the cylinder surface of them. A magnified SEM image of Cu_2O NWs is displayed in Figure 1b. A marked single Cu_2O NW has a straight shape, and a rough surface with the diameter about 123 nm. A low-magnification

transmission electron microscope (TEM) image of a typical Cu_2O NW is shown in Figure 1c. As seen from Figure 1c, a single Cu_2O NW shows a light roughness on its top side, which agrees with the surface of Cu_2O NWs displayed in the SEM image. Its average diameter is ~95 nm. The corresponding high-resolution TEM (HRTEM) image marked with the white dashed line and the corresponding selected area electron diffraction (SAED) pattern are shown in Figure 1d. As seen from HRTEM image, the distance between two adjacent crystal planes is 0.214 nm. The SAED pattern also suggests a good crystalline quality of Cu_2O NW.

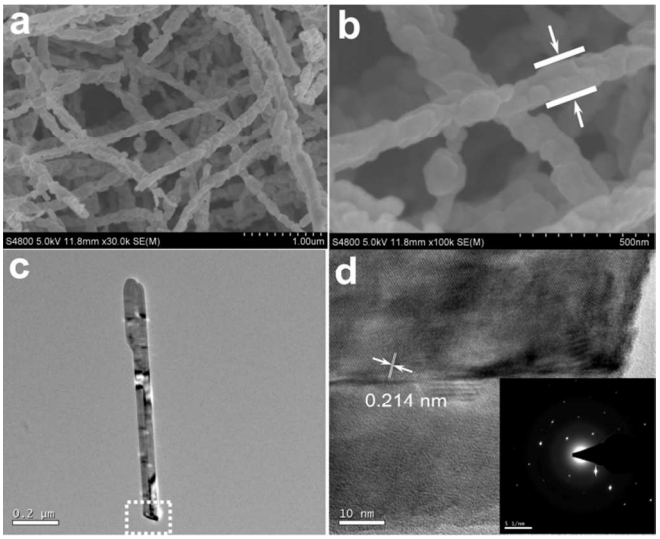

Figure 1 Electron micrographs of Cu_2O NWs. (a) Top view scanning electron microscope (SEM) image of the Cu_2O NWs. (b) A high-magnification SEM image of as-fabricated Cu_2O NWs. (c) Transmission electron microscope (TEM) image of a single Cu_2O NW. (d) A corresponding high-resolution TEM (HRTEM) image of the same Cu_2O NW marked by dashed lines in Fig. 1c, the inset shows the corresponding selected area electron diffraction (SAED) pattern of the Cu_2O NW.

Photoluminescence (PL) characterization of Cu_2O NWs was performed using UK Edinburgh Instruments FLS920 Fluorescence Spectrometer. Figure 2 plots the room temperature PL excitation and emission spectra of Cu_2O NWs. The room-temperature excitation spectrum is depicted in Figure 2a. As is seen from the spectrum, the excitation peak of Cu_2O NWs is ~380 nm, and the range of the optimum excitation wavelength for Cu_2O NWs is from 350 to 390 nm. The excitation wavelength of 360 and 380 nm are chosen in order to compare the difference of exciton emission in Cu_2O NWs. Figure 2b shows the room temperature PL spectrum of Cu_2O NWs under excitation wavelength of 360 and 380 nm. Noted that the PL intensity is dependent on the excitation wavelength and the maximum emission peak of PL spectra is at the wavelength of 532 nm (i.e. 2.33 eV, denoted as main line), which is independent on the excitation wavelength. It almost corresponds with the value of the Cu_2O band-gap energy at the Γ point in previous reported work [14]. Thus the result demonstrates the PL peak at the wavelength of 532 nm is due to the near band edge (BE) emission of the sample. The absence of distinct weak peak in Figure 2b also indicates that the PL emission is dominated by radiative recombination from BE exciton located at 2.33 eV at room temperature. To further investigate the PL emission depended on the time for the Cu_2O NWs, the PL decay curve collected at the excitation wavelength of 360 nm was measured at room temperature, as depicted in Figure 2c. The non-exponential decay is observed and can be fitted to a multi-exponential decay function with IRF curve, indicating three lifetime components (i.e., short lifetime, long lifetime, and longer lifetime). The three lifetime components illustrate the exciton dynamics of the Cu_2O NWs, yielding a short lifetime τ_s, a long lifetime τ_{L1}, and a longer lifetime τ_{L2}. The lifetime τ_s, τ_{L1}, and τ_{L2} are 0.71, 2.86, and 8.94 ns, respectively. All of which reflect the information of the fine structure of exciton in Cu_2O NW. This subject is beyond the scope of this work and will be discussed later.

To illustrate the deeper insight of the exciton dynamics of the Cu_2O NWs at the peak of the PL spectrum, a time-resolved PL measurement is performed as a function of temperature, as shown in Figure 2d. Through fitting the decay curves, the result shows the temperature depended PL decay curves have still three lifetime components. As shown in Figure 2d, the lifetime τ_s and τ_{L1} are 0.78 and 2.82 ns by fitting the curves using the software of the instrument, respectively, almost keeping unchanged as the temperature below 200 K. It is noted that the τ_{L2} slightly increase from 200 to 77 K, rising from 8.70 to 8.79 ns. This implies the lifetimes τ_{L2} component becomes longer by suppressing the nonradiation decay in Cu_2O NWs at low temperature, showing that it is a temperature-activated process.

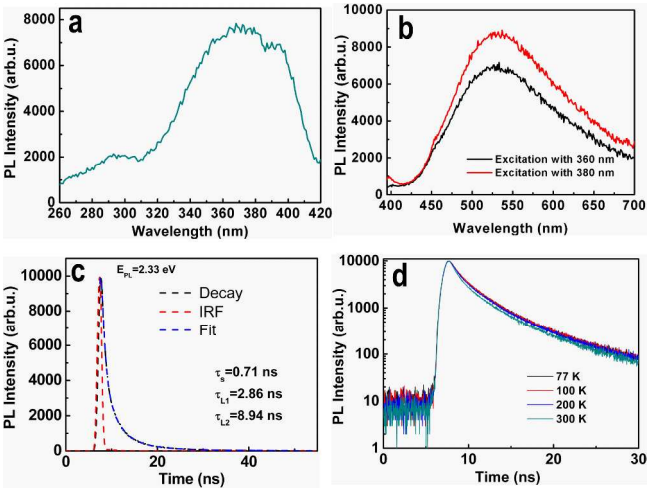

Figure 2 PL spectra of the as-synthesized Cu_2O NWs. (a) PL excitation spectrum of the Cu_2O NWs at room temperature. (b) PL spectra of the Cu_2O NWs under the excitation wavelength with 360 and 380 nm at room temperature. (c) PL decay of the Cu_2O NWs recorded at the emission of 2.33 eV at room temperature. (d) PL decays of the Cu_2O NWs in semi-log y scale as a function of temperature from 77 to 300 K at the emission of 2.33 eV.

In order to demonstrate the characteristics of the BE emission from the sample, the temperature dependent PL experiments are performed, as reported in Figure 3. First, the PL experiments of the Cu_2O NWs depended on temperature ranged from 77–300 K are performed under the excitation wavelength of 360 nm, as shown in Figure 3a. The intensity of the main emission line increases as the temperature decrease from 300 to 77 K, and that of the main line obviously remains unchanged in the temperature range of 77 to 250 K. This is due to its same parity of conduction and valence bands, the low band-to-band transition efficiency prevents them from high intensity light emission [17]. Furthermore, the intensity of the main line at 300 K reaches its minimum within the whole temperature range. The decrease probably arises from nonradiative

recombination in the sample. It is also noted that a blue shift of PL main peak is observed with decreasing temperature to 77 K, reaching its maximum of 35.9 meV, the blue shift of BE emission mainly arises from the suppression of the nonradiative recombination. Specifically, five new emission lines depicted in Figure 3a (denoted as E_A, E_C, E_D, A, and B) include three stronger lines (E_A, A, B) and two weak lines (E_C, E_D) for every curve at the temperature lower than 250 K. At the temperature below 250 K, a sharp emission line with 2.36 eV (i.e., the line B) appears. And the sharp emission line shows the FWHM (Full width at half maximum) of ~9 nm. The intensity of another emission line E_A at the energy of 1.965 eV (i.e., 631 nm) almost keeps constant when temperature changes from 100 to 250 K, whereas its intensity reaches the maximum at 77 K. The line E_A is close to the reported exciton peak with 1S of E_{OA} (2.02 eV) [14], the energy difference between them is 55 meV. It might be attributed to the first-order longitudinal optical (LO) phonon replica of 1S of E_{OA}. This would be discussed below. The lines E_C (2.638 eV) and E_D (2.755 eV) are close to the reported exciton peaks with E_{OC} and E_{OD} whose value are 2.624 and 2.755 eV [14]. Simultaneously, the high energy line A (3.084 eV) should possibly be associated with interband transitions rather than the intra-atomic properties of impurities or defects [14]. Herein, we focus on the visible part with energy below 3.0 eV, which should reflect the information on the exciton properties near the band edge. Most notablely, when the temperature is up to 300 K, the five lines entirely disappear. Next, the origin of the lines should be discussed in detail.

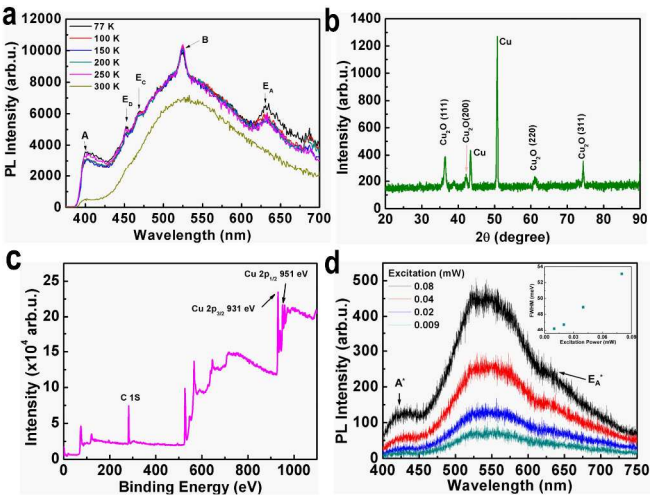

Figure 3 (a) PL spectra of the prepared Cu_2O NWs as a function of temperature from 77 to 300 K. (b) XRD spectrum of the Cu_2O NWs. (c) Wide scan XPS spectrum of the prepared Cu_2O NWs. (d) Micro-region PL spectra of the Cu_2O NWs as a function of pump intensity of a He-Cd laser with 325 nm at room temperature.

In order to justify the origin of the line B, we propose two hypotheses to explain the appearance of the sharp emission line. First, the line probably results from the emission of impurity in Cu_2O NWs. Second, it demonstrates efficient spontaneous emission of exciton can take place in Cu_2O NWs. In the following, we would test each of the hypotheses mentioned above.

First, we test the hypothesis of the presence of defects or impurity in Cu_2O NWs. The X-ray powder diffraction (XRPD) measurement was firstly carried out by using a Rigaku Corporation D/Max-2400 to detect the crystalline quality of sample. Figure 3b displays the XRPD patterns of the Cu_2O NWs samples. No peaks from CuO are presented, and no impurity peaks are observed in this pattern. Besides XRPD spectrum, x-ray photoelectron spectroscopy (XPS) spectrum of the Cu_2O NWs sample is performed by using a Kratos AXIS Ultra^{DLD} under room temperature, as shown in Figure 3c. The full spectrum indicates that Cu and O are the pure constituents of the sample, with C as reference. In addition, two distinct peaks are observed and marked in Figure 3c at 931 and 951 eV, corresponding to the binding energy of Cu $2p_{3/2}$ and Cu $2p_{1/2}$. The results are in agreement with previous report [18] on Cu_2O NWs. Based on these facts, Cu_2O NWs sample can be assumed to have no impurity.

Then the pump intensity dependent micro-region PL spectra of the Cu_2O NWs were conducted using a HORIBA LabRAMHR800 Raman spectrometer for testing the efficient spontaneous emission of exciton. The sample was optically pumped by a He-Cd laser with 325 nm at room temperature. We adjusted the excitation power by ~1 order of magnitude, and the corresponding PL spectra are shown in Figure 3d. It is noted that, under different excitation densities, the shape and the position of main emission peak with 2.36 eV almost remain unchanged. Besides, the FWHM of the main emission peak shows almost linear relationship with excitation power, as shown in the inset of Figure 3d. According the previous investigations on the exciton emission in Cu_2O [14], the main emission peak with 2.36 eV is close to the lowest direct bandgap peaks of E_{0B} (2.43 eV) in Cu_2O thin film. So it arises from the radiative recombination of E_{0B}. Furthermore, the high energy side and low energy side of the PL spectra have a different response as the excitation power increased. When excitation power is larger than 0.02 mW, two weak emission lines of A^* and E_A^* with 2.85 and 1.96 eV occur. Arising from the weak exciton states, the two lines are possibly related with the E_{OD} and the 1S of E_{OA} in the previous report [14]. In this work, the line of E_D has been recorded in Figure 3a. Compared with the E_D of 2.755 eV at low temperature, there is slightly blue-shifted for A^* at room temperature. One possible explanation for that is the line A^* reflects the emission information of a few Cu_2O NW, which manifest the optical feature in the reduced dimensionality. We estimate the number of Cu_2O NW in the area with ca. 3 μm^2 (i.e., the area of lighting spot recorded by the micro-region PL spectrometer), the value is approximately 7. So we conclude the lines E_D and A^* arise from the same exciton states. In order to demonstrate the emission from Cu_2O NWs, a PL microscope image from the same sample is shown in Figure 4. A white light spot with the diameter of ~2 μm is clearly observed, indicating efficient radiation can take place in Cu_2O NWs. The white light assigns to the mixture of three emission lines, which is the main line, the line A^*, and the line E_A^*.The three emission lines just correspond to green, blue, and red lights.

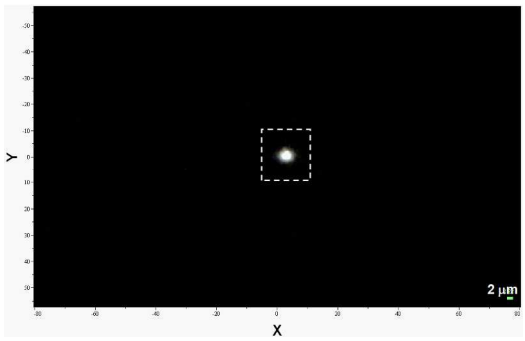

Figure 4 A optical image of the emitted light spot from the prepared Cu_2O NWs recorded by a Micro-region Raman spectrometer.

In Figure 3d, the energy of the line E_A^* is the same as that of the E_A in Figure 3a. We conclude the low energy line E_A^* is highly related with phonon-assisted emission. In order to further justify the line E_A^* attributing to the direct exciton combination with or without phonons participation, or defect related emission. The PL decay experiment for the line E_A^*, B, and main line is first performed at 77 K, as depicted in Figure 5. In Figure 5, the lifetime of the sample demonstrates the discrepancy for the three emission lines (i.e. B, E_A, and the main line) at the temperature of 77 K. Most strikingly, the lifetime τ_s, τ_{L1}, and τ_{L2} of the main line is the longest among the three lines, reaching 0.78, 2.82, and 8.79 ns, respectively. While the lifetime of lines B and E_A show distinctly shorter than that of the main line. It implies the other two peaks aren't from the defect related emission. Because defects have longer fluorescence lifetimes than band edge recombinations [19]. Thus, the lifetime τ_s, τ_{L1}, and τ_{L2} represent the radiative recombination of exciton in the Cu_2O NWs.

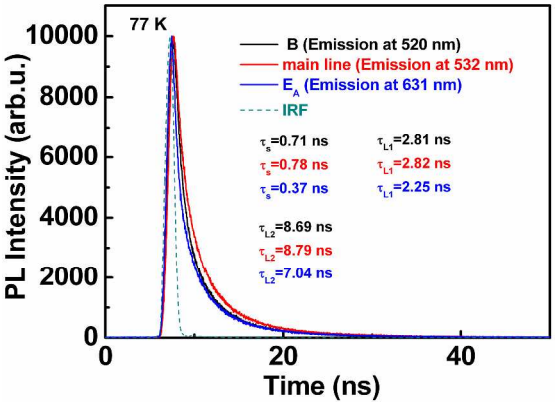

Figure 5 PL decays of Cu_2O NWs with the emission of 2.36, 2.33, and 1.965 eV (i.e., 520, 532, 631 nm) at the temperature of 77 K, τ_s, τ_{L1}, and τ_{L2} characterize the three lifetime components of the Cu_2O NWs.

According to the report by Dawson *et al.*[20], the LO phonon with energy 78.7 meV was obtained for Cu_2O. The line E_A^* is close to the peak from 1S of E_{OA}. But the recombination from the E_{OA} is dipole-forbidden [14], thus we conclude the appearance of the line E_A^* arises from direct band edge emission with phonon-assisted. In order to test the hypothesis that the line E_A^* could be the exciton recombination with phonon-assisted. A general relationship of the emission line involving phonons and the exciton emission should be given as, $E_{em}= E_0-n\hbar\omega_{LO}+\Delta E$ [21], E_{em} denotes the energy of emission peak,E_0 is the excitonic absorption peak energy. LO phonon energy is denoted $\hbar\omega_{LO}$ and ΔE is the thermal energy. At room temperature, $\Delta E= kT/2 \approx 13$ meV. Therefore, the exciton peak from the 1S of E_{OA} is about 2.02 eV, the calculated value of 1S of E_{OA} with phonon replicas is ~1.954 eV, which is in good agreement with our experiment observation of 1.96 eV mentioned above. Therefore, we conclude the line E_A^* can be attributed to the first-order LO phonon replica of 1S of E_{OA}.

Conclusions

In conclusion, we have fabricated Cu_2O NWs with the bulges on the surface of them. The exciton optical properties near the band edge of the Cu_2O NWs have been characterized by detailed analysis of temperature and excitation intensity-dependent PL spectra. Different exciton emission lines of Cu_2O NWs are observed. Furthermore, the emission from the first-order LO phonon replica of exciton with dipole forbidden can be observed for the first time. The experimental result about the LO phonon replica is in good agreement with calculated value. Notably, we can observe a visible light emission from the Cu_2O NWs at room temperature. These results will be potentially helpful to optimize the exciton emission efficiency by tailor exciton−phonon coupling strength, and further improve phonon anticipated exciton thansport process. Our study would not only advance the understanding of exciton optical properties in Cu_2O NWs, but will pave the way for efficient excitonic emission devices based on Cu_2O NWs at room temperature.

Acknowledgments

The authors thank Dr. Cheng Liu, A/Prof. Qing Su, and Zhenghua Ju for assistance in PL measurements. This work was supported by the National Natural Science Foundation of China (Grants 61204106) and the foundation of State Key Library of Functional Materials for Informatics (Shanghai Institute of Microsystem and Information Technology).

Notes and references

[a]School of Physical Science and Technology, Lanzhou University, Lanzhou 730000, China. E-Mail: wangpeng@lzu.edu.cn

[b]Department of Optical Information Science and Technology，School of Mechanical Engineering， Jiangsu University， Zhenjiang 212013, China.

[c]OriginLab (Guangzhou) Ltd., No. 109 Tiyuxi Road, Guangzhou 510620, China.

[d]Maternity & Child-care Hospital of Gansu province,Lanzhou, 730050, China.

† Electronic Supplementary Information (ESI) available: The decay curves in semi-log y scale in Figure 2c and 5, a diameter distribution diagram of the prepared Cu_2O NWs, and a high-resolution Transmission electron microscope (HRTEM) image of the same Cu_2O NW with that in Figure 1d should been shown in the Electronic Supplementary Information. See DOI: 10.1039/b000000x/

1.Talia Gershon, Kevin P. Musselman, Andrew Marin, Richard H. Friend, and Judith L. MacManus-Driscoll, Sol. Energy Mater. Sol. Cells, 2012, 96, 148.

2.Markus Heinemann, Bianca Eifert and Christian Heiliger, Phys. Rev. B, 2013, 87, 115111.

3. Li Zhang and Hui Wang, ACS Nano, 2011, 5, 3257.

4. Chengxiang Xiang, Gregory M. Kimball, Ronald L. Grimm, Bruce S. Brunschwig, Harry A. Atwater, and Nathan S. Lewis, Energy Environ. Sci., 2011, 4, 1311.

5.Kevin P. Musselman, Andrew Marin, Lukas Schmidt-Mende, and Judith L. MacManus-Driscoll, Adv. Funct. Mater., 2012, 22, 2202.

6. N. Naka and N. Nagasawa, Phys. Rev. B, 2002, 65, 245203.

7. David Snoke, Science, 2002, 298, 1368.

8. Conghua Lu, Limin Qi, Jinhu Yang, Xiaoyu Wang, Dayong Zhang, JinglinXie, and Jiming Ma, Adv. Mater., 2005, 17, 2562.

9.Chun-Hong Kuo and Michael H. Huang, J. Phys. Chem. C, 2008, 112, 18355.

10.Zheng Liu, Yongjie Zhan, Gang Shi, Simona Moldovan, Mohamed Gharbi, Li Song, Lulu Ma, Wei Gao, Jiaqi Huang, Robert Vajtai, Florian Banhart, Pradeep Sharma, Jun Lou, and Pulickel M. Ajayan, Nat. Commun. 2012, 3, 879.
11.Li Zhang, Douglas A. Blom and Hui Wang, Chem. Mater., 2011, 23, 4587.
12.Zhonghai Zhang, RubalDua, Lianbin Zhang, Haibo Zhu, Hongnan Zhang, and Peng Wang, ACS Nano 2013, 7,1709.
13.Guangliang Cui, Mingzhe Zhang and Guangtian Zou, Scientific Reports, 2013, 3, 1250.
14.Jun-Woo Park, Hyungkeun Jang, Sung Kim, Suk-Ho Choi, Hosun Lee, Joongoo Kang, and Su-Huai Wei, J. Appl. Phys., 2011, 110, 103503.
15.Peng Wang, Xinhong Zhao and Baojun Li, Opt. Express, 2011, 19, 11271.
16.Guofu Ma, Su Liu, Peng Wang, Jingxian Chang, Miao Zhang, and Hairong Li, Materials Letters, 2014, 120, 212.
17.Shu Sheng Pan, Siu Fung Yu, Wen Fei Zhang, Hai Zhu, Wei Lu and Li Min Jin, Nanoscale, 2013, 5, 11561.
18.Xiaoyan Liu, Renzhi Hu, Shenglin Xiong, Yankuan Liu, Lanlan Chai, Keyan Bao, and Yitai Qian, Mater. Chem. Phys. , 2009, 114, 213.
19.Mickaël D. Tessier, Louis Biadala, Cécile Bouet, Sandrine Ithurria, Benjamin Abecassis, and Benoit Dubertret, ACS Nano, 2013, 7, 3332.
20.P. Dawson, M. M. Hargreave and G. R. Wilkinson, J. Phys. Chem. Solids, 1973, 34, 2201.
21.S. Chakraborty and P. Kumbhakar, Materials Letters, 2013, 100, 40.